Closed-Loop Kinematic Calibration of the RSI 6-DOF Hand Controller

John M. Hollerbach, *Senior Member, IEEE*, and David M. Lokhorst

***Abstract*— A method is presented for autonomous kinematic calibration of the RSI 6-DOF hand controller, a two-loop parallel mechanism comprised of three 6-DOF arms with potentiometers on the first three joints of each arm. This double closed-loop kinematic calibration method is an adaptation of a previously developed single closed-loop method. The kinematic parameters identified are the joint angle offsets and the joint angle gains. Experimental results are presented and compared to results using a special calibration fixture.**

I. Introduction

RECENTLY, it has been shown that single-loop closed chains can be kinematically calibrated using joint angle readings alone [3]. The closed chain must be mobile, and no more than five of the joints may be unsensed in the general case. By placement of the closed chain into a number of configurations, consistency conditions permit the kinematic parameters to be extracted. In this paper, the closed-loop method is extended to a multiple loop mechanism, the RSI 6-DOF hand controller.

Applications of the closed-loop method are beginning to appear. For single loops, in [2] experimental results were presented for closed-loop calibration of the Utah/MIT Dextrous Hand. In [15], a line constraint was defined by a laser, which was tracked using an endpoint retroreflector on a PUMA 560 and a 4-quadrant detector. In [7], a fiducial point on the end effector is touched to a fiducial point on the environment in several different poses; this corresponds to the point contact case in [3]. In [13], a teleoperated excavator with unsensed joints was calibrated by adding an additional linkage (called a calibrator by the authors) with some sensed joints to form a closed loop. In [9], a ball bar with fixed length and unsensed spherical joints at each end was employed.

In [4], it was shown that the closed loop did not need to involve physical linkages, but could be formed by optical paths as virtual limbs to a stereo camera system. An uncalibrated stereo camera system could be simultaneously calibrated with an uncalibrated manipulator. Closed-loop calibration of a manipulator with a camera mounted on an end effector was presented in [21]. In [20] it was shown how a 4-beam laser tracking system could be calibrated by a closed loop method.

When optical paths are viewed as limbs, the systems in [4], [20] can be regarded as multiple-loop kinematic chains. Boulet [6] applied closed-loop calibration to a mechanical two-loop system formed as a single joint with two antagonistic linear actuators. Wampler and Arai [19] proposed an extension of the single-loop method to arbitrary multiple loops; simulations were presented for a two-loop planar mechanism comprised of three prismatic legs with passive rotary joints at their ends attached to a triangular stage.

In this paper, the closed loop approach is adapted to a double-loop mechanism, the RSI 6-DOF hand controller (Fig. 1). This hand controller is a positioning master, and involves manipulation of a handle in a range of ± 3 in. in X, Y, and Z, and $\pm 30°$ in roll, pitch, and yaw. The handle is attached to a base by three identical 6-DOF arms, each of which is comprised of a rotary shoulder joint, a Hookean elbow joint, and a spherical wrist. There are potentiometers at the shoulder and elbow joint, but the wrist joints are unsensed.

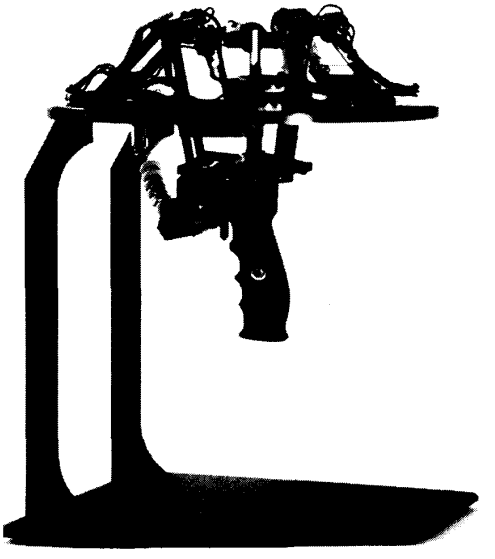

Fig. 1 The RSI 6-DOF hand controller.

Manuscript received March 22, 1993; revised August 11, 1993. This work was supported by the Office of Naval Research Grant N00014-90-J-1849, and by the Natural Sciences and Engineering Research Council (NSERC) Network Centers of Excellence Institute for Robotics and Intelligent Systems (IRIS). Support for J. M. Hollerbach was provided by the NSERC/Canadian Institute for Advanced Research (CIAR) Industrial Research Chair in Robotics.

J. M. Hollerbach was with the Departments of Mechanical Engineering and Biomedical Engineering, McGill University, Montreal, Quebec H3A 2B4, Canada. He is now with the Department of Computer Science, University of Utah, 3190 Merrill Engineering Building, Salt Lake City, UT 84112 USA.

D. M. Lokhorst is with RSI Research Ltd., 10-10114 McDonald Park Road, Sidney, British Columbia V8L 3X9, Canada.

IEEE Log Number 9410121.

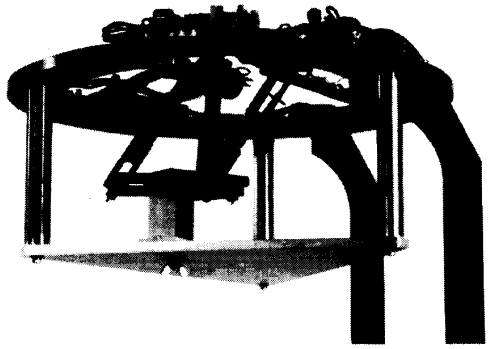

Fig. 2 A calibration fixture replaces the handle and attaches to the arms.

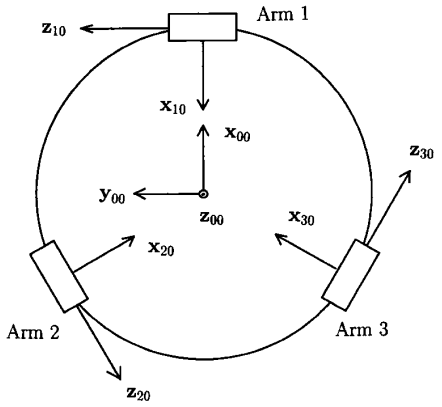

z_{ij} is the rotation axis embedded in link ij at the distal joint $i, j+1$.
x_{ij} is defined along the common normal from $z_{i,j-1}$ to z_{ij}. The common normal's intersection with z_{ij} defines the location of joint $i, j+1$.
s_{ij} is the distance along $z_{i,j-1}$ from $x_{i,j-1}$ to x_{ij}.
a_{ij} is the distance along x_{ij} from $z_{i,j-1}$ to z_{ij}.
α_{ij} is the skew angle about x_{ij} from $z_{i,j-1}$ to z_{ij}.
θ_{ij} is the rotation angle about $z_{i,j-1}$ from $x_{i,j-1}$ to x_{ij}.

Fig. 3 Top plate viewed from above, showing base coordinate system and attachments of arms.

Given that the specification on accuracy in handle placement is $\pm 1\%$, there is not a requirement to identify kinematic parameters associated with length or with relative orientation of neighboring joint axes. The machining and fabrication processes may be presumed to be precise enough to yield a real mechanism close enough to the design to achieve this level of accuracy. However, because of analog electronics associated with the use of potentiometers, the joint angle offsets and joint angle gains need to be calibrated initially and then periodically recalibrated over time.

A special calibration fixture was devised for this hand controller. In order to use this fixture, the handle is removed from the arms and the fixture is inserted in its place (Fig. 2). This fixture is then moved to 12 mechanically predetermined poses.

With this fixture, it is not practical to recalibrate the hand controller in the field. It would be desirable to have an automatic calibration method that does not require a fixture, such as the single closed-loop calibration method [3]. To eliminate the unsensed wrist joints, we use the constraint that the distance between any pair of wrist joints is a known constant. These three pairwise constraints form an adequate basis for autonomous calibration of the desired kinematic parameters of the RSI hand controller, i.e., the joint angle offsets and the joint angle gains. A requirement of this method is that the nominal parameters are within 10% of the actual parameters. Hence this method is well suited towards recalibration, because it may be presumed that the parameter drift over time is slow.

The 10% accuracy requirement for the nominal parameters is due to a problem in identifying the joint angle gains. Previously it was shown that when the closed single-loop calibration method was applied to determine the joint angle gains, there is a strong attraction in the nonlinear optimization stage to a trivial solution of all zero gains [2]. To overcome this problem, one of the gains was presumed known and treated as a constant; calibration could then proceed robustly as before. In practice, it is not feasible to determine or to presume as known one of the gains. Fortunately, we have found in the present approach that there is a small region of attraction to the correct solution, roughly when the nominal values are within 10%. The attraction region is highly dependent on the set of poses chosen.

In the rest of the paper, the mechanism's kinematics are first presented and then the double closed-loop method is discussed. Experimental results are shown for this closed-loop method, and are compared to results using the calibration fixture. An initial presentation of this work appeared in [12].

II. Mechanism Kinematics

A double-subscripted form of the Denavit-Hartenberg (DH) parameters [8] is employed to describe the hand controller's kinematics. The three arms are attached to a top plate at equal spacings of 120° (Fig. 3) around a circle, and are numbered clockwise from 1 to 3 as viewed from above. The DH parameters for arm i are described by subscript ij.

A global base coordinate system numbered 00 is placed in the middle of the top plate, so that z_{00} is normal to the top plate and pointing upwards, and x_{00} is directed towards the arm 1 attachment point. Each arm base axis z_{i0} lies in the plane of the top plate, is tangent to the hypothetical circle connecting the arm attachment points, and is counterclockwise in direction as viewed from above. Each x_{i0} axis also lies in the top plate, and is directed towards the 00 coordinates.

The DH parameters for the global base and the first three DOFs of the arms are presented in Table I. The joint variables for the arms are θ_{ij} for $j = 1, 2, 3$, while the parameters θ_{i0} express a fixed relation of the arm bases to the global base. For each arm, the first two joints form a planar two-link manipulator, while the third joint forms a Hookean joint with

TABLE I
DH PARAMETERS FOR EACH ARM i

j	a_{ij} (in)	s_{ij}	a_{ij} (rad)	i	θ_{i0} (rad
0	-4.5	0.0	$\pi/2$	1	π
1	3.2	0.0	0	2	$\pi/3$
2	0.0	0.0	$\pi/2$	3	$-\pi/3$
3	0.0	0.0	0		

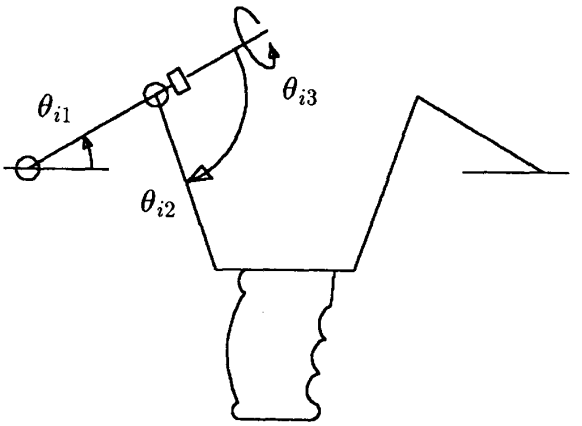

Fig. 4 Joint limits for a typical linkage. θ_{i1}: -90° to +90°, θ_{i2}: 0° to -180°, θ_{i3}: -90° to +90°.

the second. Fig. 4 shows the structure of arm i, and indicates the joint limits.

The wrist DOFs are unsensed, and must be eliminated from any calibration equations. In the calibration method described in Section III, we require only the location of the wrist points and not the wrist angles themselves. Hence we do not develop DH parameters for the wrist DOFs. Each wrist point is located by the axis x_{i3}, and is a distance $l_3 = 3.971$ from the elbow point. We will also use the notation $l_1 = a_{i0}$ and $l_2 = a_{i1}$.

The wrists of the three arms are attached to the top plane of a handle, equally spaced at 120° intervals on a circle (Fig. 5), in a clockwise direction from wrist 1 to wrist 3 as viewed from above. The handle coordinates, subscripted H, are placed at this circle's center such that z_H points upwards and x_H is directed towards wrist 1's attachment point (Fig. 5). The distance from the center to each wrist point is $l_4 = 1.5$.

A. Forward Kinematics

In forward kinematics, the pose of the handle is found from the joint angles. Although 6 joint angle sensors are the theoretical minimum required to solve the forward kinematics, multiple solutions arise which are unacceptable in practice [17]. Even 8 sensors yield multiple solutions. Hence the current design utilizes 9 sensors in the configuration described above, to yield a unique handle pose given the joint angles.

The position of the handle origin O_H relative to the top plate base origin O_B (Fig. 6) is located by the vector r_H (Fig. 5), and the orientation of the handle axes $\mathrm{x}_H, \mathrm{y}_H, \mathrm{z}_H$ relative to the base axes $\mathrm{x}_{00}, \mathrm{y}_{00}, \mathrm{z}_{00}$ is specified by the RPY Euler angles $(\theta_x, \theta_y, \theta_z)$, where

$$[\mathrm{x}_H \mathrm{y}_H \mathrm{z}_H] = \mathrm{R}_z(\theta_z)\mathrm{R}_y(\theta_y)\mathrm{R}_x(\theta_x) \tag{1}$$

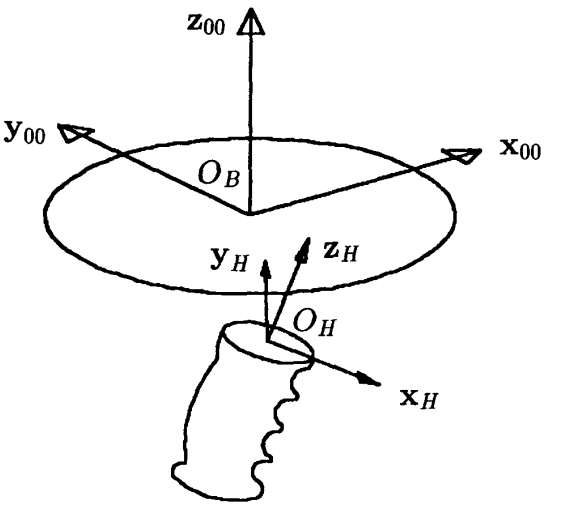

Fig. 5 Handle coordinates $\mathrm{x}_H, \mathrm{y}_H, \mathrm{z}_H$ are fixed in the middle of the top plate of the handle. Vector r_i locates wrist i relative to the top plate base origin O_B, and vector r_H locates the handle origin O_H relative to O_B.

and R_z is a rotation about the z axis, etc. Let r_i be the position of wrist i. The forward kinematics to find r_i are straightforward through the use of the DH homogeneous transformations A_{ij}, which for arm i expresses the transformation from coordinate systems ij to $i, j-1$. An intermediate result for r_{i0}, the vector from coordinate system $i0$ to wrist i expressed in the $i0$ coordinates, will be useful in the next subsection.

$$\mathrm{r}_{i0} = \begin{bmatrix} l_2 \cos\theta_{i1} + l_3 \cos(\theta_{i1} + \theta_{i2}) \cos\theta_{i3} \\ l_2 \sin\theta_{i1} + l_3 \sin(\theta_{i1} + \theta_{i2}) \cos\theta_{i3} \\ l_3 \sin\theta_{i3} \end{bmatrix}$$
$$\begin{bmatrix} \mathrm{r}_i \\ 1 \end{bmatrix} = \mathrm{A}_{i0} \begin{bmatrix} \mathrm{r}_{i0} \\ 1 \end{bmatrix} \tag{2}$$

where A_{i0} is the transformation from coordinate system $i0$ to 00 (see Fig. 3). The handle position r_H is simply found as

$$\mathrm{r}_H = \frac{1}{3}(\mathrm{r}_1 + \mathrm{r}_2 + \mathrm{r}_3) \tag{3}$$

The handle axes are found as

$$\mathrm{x}_H = \frac{1}{l_4}(\mathrm{r}_1 - \mathrm{r}_H)$$
$$\mathrm{y}_H = \frac{2}{l_4\sqrt{3}}(\mathrm{r}_3 - (\mathrm{r}_3 - \mathrm{r}_2)/2) \tag{4}$$

and $\mathrm{z}_H = \mathrm{x}_H \times \mathrm{y}_H$. The RPY Euler angles may be extracted from (1) by standard procedures [16].

$$\theta_z = \mathrm{atan}(x_H(2)/x_H(1))$$
$$\theta_y = \mathrm{atan2}(y_H(3), z_H(3)) \tag{5}$$
$$\theta_x = \mathrm{atan2}(x_H(3), x_H(1)\cos\theta_z + x_H(2)\sin\theta_z)$$

where $x_H(2)$ is the second component of vector x_H, etc., and atan2 is the four-quandrant arctangent function.

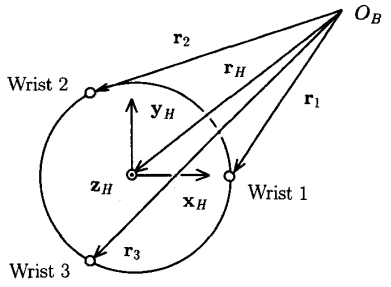

Fig. 6 Handle coordinates x_H, y_H, z_H are related to the top plate base coordinates x_{00}, y_{00}, z_{00}.

B. Inverse Kinematics

Given r_H and $(\theta_x, \theta_y, \theta_z)$, the goal is to find the joint angles θ_{ij}. Let $\mathbf{q}_i$ be a vector from the handle center to wrist point i, expressed in the handle coordinates. Then the wrist points $\mathbf{r}_i$ are located as

$$\mathbf{r}_i = \mathbf{r}_H + \mathbf{R}\mathbf{q}_i$$

where the rotation matrix R is the result of evaluating (1). Then $\mathbf{r}_{i0}$ is found by inverting (2). From (2),

$$\theta_{i3} = \sin^{-1}\left(\frac{r_{i0}(3)}{l_3}\right) \tag{6}$$

This puts θ_{i3} in quadrants I or IV, in accordance with the joint limits (Fig. 4).

We are now left with a planar 2-link manipulator problem. The solution for θ_{i2} is

$$\theta_{i2} = \cos^{-1}\left(\frac{r_{i0}(1)^2 + r_{i0}(2)^2 - l_2^2 - l_3^2\cos^2\theta_{i3}}{2l_2 l_3 \cos\theta_{i3}}\right) \tag{7}$$

where the result is placed in quadrants III or IV (see Fig. 4). The joint limits shown in Fig. 4 are considerably greater than the normal working range, which is approximately ± 0.7 radians for joint θ_{i2} and -1.0 to -2.2 radians for joint θ_{i3}. Hence the inverse sine and cosine functions are well behaved. Finally,

$$\theta_{i1} = -\cos^{-1}\left(\frac{r_{i0}(1)^2 + r_{i0}(2)^2 + l_2^2 - l_3^2\cos^2\theta_{i3}}{2l_2\sqrt{r_{i0}(1)^2 + r_{i0}(2)^2}}\right) + \tan^{-1}\left(\frac{r_{io}(2)}{r_{io}(1)}\right) \tag{8}$$

III. Closed-loop Calibration Procedure

As mentioned in the Introduction, the parameters to be calibrated are the joint angle offsets θ_{ij}^{off} and the joint angle gains k_{ij}, which relate the raw analog input data α_{ij} from the potentiometers (0 to 4096 counts) to the joint angles θ_{ij}:

$$\theta_{ij} = k_{ij}\alpha_{ij} + \theta_{ij}^{off} \tag{9}$$

for joints $j = 1, 2, 3$ and arms $i = 1, 2, 3$.

For the closed-loop calibration, the handle is manually moved into a number of poses by the operator, and at each pose the joint angles are read. With this information alone, calibration may proceed because of the basic observation that the displacement around each of the two closed chains must be zero. However, we cannot proceed exactly this way because the wrist joints are unsensed and must not appear in the calibration equations. The simplest way to formulate calibration equations without wrist joints is to note that the distance between any two pairs of wrist points is constrained to be a constant, $d = l_4\sqrt{3}$. The resulting three constraints for every pairwise combination of wrist points are an adequate basis for calibration.

Suppose that the hand controller is placed into p poses, and let $\mathbf{r}_i^m$ be the location of wrist i in pose m. Define the $3p$-dimensional error vector f with the following components:

$$\begin{aligned} f(3m-2) &= (\mathbf{r}_1^m - \mathbf{r}_2^m)^2 - d^2 \\ f(3m-1) &= (\mathbf{r}_2^m - \mathbf{r}_3^m)^2 - d^2 \\ f(3m) &= (\mathbf{r}_1^m - \mathbf{r}_3^m)^2 - d^2 \end{aligned} \tag{10}$$

where $m = 1, \ldots, p$. Then calibration can be performed by solving the following least squares problem:

$$\min_{\theta_{ij}^{off}, k_{ij}} \mathbf{f}^T\mathbf{f} \tag{11}$$

The solution can be accomplished by the Levenberg-Marquardt algorithm, and is facilitated by providing the 18-by-3p analytic gradient g of f with components

$$\begin{aligned} g(j+3(i-1), m) &= \partial f(m)/\partial\theta_{ij} \\ g(j+9+3(i-1), m) &= \partial f(m)/\partial k_{ij} \end{aligned} \tag{12}$$

for $j = 1, 2, 3$, $i = 1, 2, 3$, and $m = 1, \ldots, 3p$. The evaluation of the gradient is straightforward and is omitted.

IV. Results

In this section, we present initially the experimental results with the special calibration fixture. Next we discuss a set of simulations that were performed to assess the effects of pose selection and initial parameter error on the convergence of the proposed method. Finally, experimental results for the proposed closed-loop method are presented and compared to those obtained with the fixture.

A. Experimental Results Using the Special Calibration Fixture

During the calibration procedure, the handle is removed and is replaced by a mechanical fixture (Fig. 2). This fixture has mechanical stops and adjustments, which allow the arms to be positioned corresponding to the 12 precise poses in Table II. The sensors used in the RSI Research 6 DOF hand controller are Midori CP-2FB precision potentiometers, which are supplied with regulated ± 5 V. Each sensor is sampled by an ADC converter, and 100 samples are averaged. The gains k_{ij} and offsets θ_{ij}^{off} are estimated by least squares estimation using MATLAB performed at the joint angle level. For each

TABLE II
CALIBRATION POSES ASSUMED BY THE FIXTURE

m	x	y	z	θ_x	θ_y	θ_y
1	0	0	-3.966	0	0	0
2	0	0	-3.966	0	0	$-\pi/2$
3	0	0	-3.966	0	0	0
4	0	0	-2.666	0	0	$-\pi/2$
5	-1.5	0	-3.966	0	0	0
6	-1.5	0	-3.966	0	0	$-\pi/4$
7	-1.5	0	-2.666	0	0	0
8	-1.5	0	-2.666	0	0	$-\pi/4$
9	0	1.5	-3.966	0	0	0
10	0	1.5	-3.966	0	0	$-\pi/4$
11	0	1.5	-2.666	0	0	0
12	0	1.5	-2.666	0	0	$-\pi/4$

TABLE III
CALIBRATION POSES FOR CLOSED-LOOP METHOD

m	x	y	z	θ_x	θ_y	θ_z
1	0	0	-1.3	$\pi/6$	$\pi/6$	0
2	0	0	-1.3	$\pi/6$	$-\pi/6$	0
3	0	0	-1.3	$-\pi/6$	$\pi/6$	0
4	0	0	-1.3	$-\pi/6$	$-\pi/6$	0
5	0	0	-1.3	$\pi/6$	0	$\pi/6$
6	0	0	-1.3	$\pi/6$	0	$-\pi/6$
7	0	0	-1.3	$-\pi/6$	0	$\pi/6$
8	0	0	-1.3	$-\pi/6$	0	$-\pi/6$
9	0	0	-1.3	0	$\pi/6$	$\pi/6$
10	0	0	-1.3	0	$\pi/6$	$-\pi/6$
11	0	0	-1.3	0	$-\pi/6$	$\pi/6$
12	0	0	-1.3	0	$-\pi/6$	$-\pi/6$

joint, the objective function to be minimized is:

$$\min_{\theta_{ij}^{off},k_{ij}} \sum_{m=1}^{p} (\theta_{ij}^{m} - k_{ij}\alpha_{ij}^{m} + \theta_{ij}^{off})^2 \tag{13}$$

where θ_{ij}^{m} is the theoretical joint angle calculated from the inverse kinematics for pose m and α_{ij}^{m} is the corresponding ADC reading. This is solved by ordinary least squares. The calibrated parameters are listed in Tables IV and V under column I.

With regard to the nominal offsets and gains used in the closed-loop estimation procedure, reference position 3 is the "rest" position, to which the hand controller returns by spring force when released. During assembly, the nine potentiometers are rotated and clamped to give a 0.00 V output (corresponding to a 2048 count ADC reading) when the hand controller is in the rest position. The electrical angle of the Midori CP-2FB potentiometer is specified as 340°. With a 12-bit ADC, the nominal gain $\hat{k}_{ij}$ is calculated simply by

$$\hat{k}_{ij} = -340^{\circ}/4096\,\text{counts} = -1.450 \times 10^{-3}\,\text{rad/count}$$

for $i, j = 1, 2, 3$. The minus sign arises because the potentiometers are connected in the negative sense. The nominal offset $\hat{\theta}_{ij}^{off}$ is calculated from (10), applied at the rest position $m = 3$:

$$\hat{\theta}_{ij}^{off} = \theta_{ij}^{3} - \hat{k}_{ij}\hat{\alpha}_{ij}^{3} \tag{14}$$

where $\hat{\alpha}_{ij}^{3} = 2048$ counts (corresponding to 0.00 V) is the value to which the potentiometer is adjusted. The results are

$$\hat{\theta}_{i1}^{off} = 3.39\,\text{rad},\ \hat{\theta}_{i2}^{off} = 1.00\,\text{rad},\ \hat{\theta}_{i3}^{off} = 2.99\,\text{rad}$$

for each arm $i = 1, 2, 3$.

B. Simulations

As mentioned in the Introduction, closed-loop calibration of the gains poses particular problems because of the strong attraction to the trivial solution $k_{ij} = 0$. From (10), it is seen that the potentiometer readings α_{ij} are multiplied by zero, and hence the data do not influence the calibration. Instead, the optimization drifts to some solution for the offsets consistent with the kinematics but not particular to any pose. In [2] where closed-loop calibration of the gains was first investigated, a solution to this problem was proposed whereby one of the gains was predetermined to anchor the solution.

TABLE IV
CALIBRATED OFFSET PARAMETERS (RAD.). I: OPEN LOOP CALIBRATION USING POSES IN TABLE II; II: CLOSED-LOOP CALIBRATION USING POSES IN TABLE III; III: CLOSED-LOOP CALIBRATION COMBINING POSES IN TABLES II-III

θ_{ij}	I	II	III
θ_{11}	3.373	3.338	3.388
θ_{12}	1.064	1.154	1.074
θ_{13}	2.847	2.869	2.862
θ_{21}	3.362	3.399	3.394
θ_{22}	1.004	1.016	0.995
θ_{23}	3.064	3.056	3.048
θ_{31}	3.363	3.365	3.370
θ_{32}	0.994	1.011	0.990
θ_{133}	3.016	3.007	3.011

For the present problem, we have found through simulation that small attraction regions exist, within roughly 10% of the correct solution for the gains, for calibrating all of the gains without presuming any to be known. To check the convergence region, the nominal joint offsets were assumed correct, while the same perturbations were added to all of the nominal joint gains. This is a more severe test of convergence than if random perturbations had been added.

The attraction region was found to be highly pose dependent. Of course pose sets can be fabricated that do not lead to convergence, if they are not sufficiently exciting. For more reasonable pose sets, a typical small convergence region for the gains relative to the nominal value of -1.45×10^{-3} was empirically found as $[-1.50,-1.40]\times10^{-3}$. A typical large convergence region was $[-1.72,-1.34]\times10^{-3}$; this pose set is the same as in Table III, except that $z = 0$. In practice, it was difficult to maneuver the handle when flush with the top plate, so a value of $z = -1.3$ was chosen. This value also places the closed-loop poses nearer the jig poses, which allows for a closer comparison. For the pose set in Table III, the convergence region was $[-1.54,-1.33]\times10^{-3}$. Looking ahead to the results in Table V, the identified gains are dispersed in the region $[-1.545,-1.411]\times10^{-3}$, so convergence was not a problem in practice.

TABLE V
CALIBRATED GAIN PARAMETERS ($\times 10^{-3}$ RAD/COUNT)

k_{ij}	I	II	III
k_{11}	-1.467	-1.445	-1.469
k_{12}	-1.496	-1.545	-1.508
k_{13}	-1.402	-1.417	-1.411
k_{21}	-1.430	-1.445	-1.439
k_{22}	-1.438	-1.451	-1.439
k_{23}	-1.473	-1.471	-1.466
k_{31}	-1.458	-1.458	-1.458
k_{32}	-1.449	-1.458	-1.449
k_{33}	-1.448	-1.441	-1.445

The convergence is relatively robust to perturbations in the poses. In simulation, random Gaussian perturbations of poses in Table III were performed with standard deviations of 0.25 in. in position and 0.25 rad in orientation. The calibration procedure converged properly under these pose perturbations. A variety of optimization methods were tried without success to extend the convergence regions, and the Levenberg-Marquardt method was retained for the experimental portion.

C. Experimental Results Using the Closed-Loop Method

The handle of the hand controller was manually placed as close as possible to the desired poses of Table III. This placement was approximate; post hoc analysis using parameter set I shows that the rms errors were 0.215 in. in position and 0.122 rad (7°) in orientation. The largest component errors for all poses were 0.571 in. and 0.435 rad (25°). Only two samples of the ADC readings were averaged for each pose, to ensure that the handle did not move noticeably during recording. Least squares optimization was performed to obtain the parameters in Tables IV and V under column II.

A better closed-loop estimate was obtained by augmenting this data set with the potentiometer readings obtained previously during open-loop calibration. After performing closed-loop calibration on the ensemble data, the parameters in Tables IV and V under column III were obtained.

The accuracy of the parameters in Tables IV and V is determined first relative to the poses and data from the calibration fixture. Using each of the three estimated parameter sets, the potentiometer readings from the jig poses are converted to predicted joint angles and predicted poses by solving the forward kinematics. These are then compared to the theoretical joint angles, found from the jig poses by solving the inverse kinematics, and the jig poses, respectively. The results are shown in Table VI. In column 1 are the rms errors in the joint angles. In columns 2-3 are the rms errors in the individual orientation components and position components. Relative to the hand controller ranges of ±30° (0.524 rad) in orientation (column 2) and ±3 in. in position, and a nominal accuracy of ±1%, then parameter sets I and III meet the accuracy requirements, while parameter set II has orientation errors which are too large.

The errors for parameter set I show how well the fixture-based calibration fits its own pose set. Ideally an independent set of poses would be chosen to compare parameters, but such a set of poses was not available. Relative to the presumed correct parameter set I, the rms errors in the closed-loop parameters II and III are shown in Table VII.

TABLE VI
RMS ERROR OF JOINT ANGLES $\psi_{\theta_{ij}}$ (RAD), ORIENTATION COMPONENTS $\psi_{\theta_{xyz}}$ (RAD), AND HANDLE POSITION COMPONENTS ψ_{xyz} (IN)

Parameters	$\psi_{\theta_{ij}}$	$\psi_{\theta_{xyz}}$	ψ_{xyz}
I	0.004	0.005	0.008
II	0.010	0.024	0.035
III	0.009	0.008	0.020

TABLE VII
RMS ERROR RELATIVE TO PARAMETER SET I OF JOINT ANGLE OFFSETS $\psi_{\theta_{ij}^{off}}$ (RAD) AND GAINS $\psi_{k_{ij}}$ ($\times 10^{-3}$) RAD COUNT

Parameters	$\psi_{\theta_{ij}^{off}}$	$\psi_{k_{ij}}$
I	0.004	0.005
II	0.010	0.024

V. DISCUSSION

We have presented an automatic procedure for kinematic calibration of the joint angle offsets and gains of the RSI 6-DOF hand controller. This closed-loop procedure requires only the joint angle sensing, and hence is a viable option for field calibration where endpoint measurement using a special calibration fixture is not feasible. This procedure is an extension of an approach initially formulated for single closed kinematic loops [3] to a double loop mechanism.

An additional development relative to previous work on single closed loops is the discovery that a small attraction region of around 10% exists for convergence of the gains to the correct values. Previously, one of the gains had to be presumed known in order to avoid the trivial solutions $k_{ij} = 0$ [2]. Hence this closed-loop procedure is best applied when a fairly good nominal parameter set is available, such as in recalibration. Simulations show that convergence is robust to perturbations of the closed-loop poses in Table III; in fact, as mentioned in the Results these poses were only approximately achieved because of manual placement.

Experimental analysis shows that the closed-loop parameter estimates are close to the open-loop parameter estimates (Table VI), but are somewhat less accurate (Table VI). More specifically, in terms of the rms errors in Table VII, the closed-loop parameter estimates III are about twice as inaccurate as the open-loop parameter estimates I. Given that the nominal accuracy of the hand controller is stated as ±1% of a ±3 in. range in position and a ±30° (0.524 rad) range in orientation, the estimates III yield component errors ψ_{xyz} and $\psi_{\theta_{xyz}}$ within the stated accuracy.

The closed-loop parameters III, determined from the combined poses, are more accurate than the closed-loop parameters II determined from the poses in Table III alone. When closed-loop calibration was performed on the jig data alone, the parameter estimates (not shown) were over 10 times worse than for parameter set III. Yet the combined data set gave a more accurate estimate than parameter set II. This range of accuracies corresponds to the observability of the poses.

TABLE VIII
THREE OBSERVABILITY MEASURES FOR DIFFERENT POSE DATA COMBINATIONS UNDER CLOSED–LOOP CALIBRATION

Observability Measure	Table II Data	Table III Data	Table II and III Data
Observability index [5]	1.01×10^{-4}	1.41×10^{-4}	1.76×10^{-4}
Condition number	920	226	95.1
Minimum singular value	9.64×10^{-6}	2.92×10^{-5}	1.04×10^{-4}

Singular values were determined from the Jacobian (13), after applying the model based column scaling in [18] to normalize for the effects of parameter errors on wrist positions; the Jacobian was evaluated with parameter set I. Three different measures of observability are shown in Table VIII: the observability index of [5], the condition number [10], and the minimum singular value [14]. For all three observability measures, the combined open plus closed-loop pose data (Tables III and IV) had the highest observability, the closed-loop pose data was intermediate, while the open-loop pose data had the lowest observability. Table VIII shows that the minimum singular value and the condition number are the most sensitive measures, varying by a factor of 10. The observability index of [5] was the least sensitive, varying by less than a factor of 2. Although pose selection was done on the basis of region of convergence, in the future one should also consider maximizing the observability.

One reason why the closed-loop method gave less accurate results than the open loop method is the lack of averaging of the readings for the closed-loop poses. For the open-loop calibration, readings were averaged 100 times at each fixture pose. For the closed-loop calibration, only 2 readings were obtained at each manually held pose because of concerns about steadiness. Table IX shows simulation results of the effect of averaging; the poses of Table III were used to generate sensor readings plus noise, using the nominal parameters to model the hand controller. Gaussian random noise with different variances was added to the simulated sensor readings, which were then rounded to the nearest integer to simulate the effect of the ADC's. Sufficient trials were done to find a stable average error for the offsets and gains. For the noise level labeled as *truncation*, the exact simulated sensor readings were rounded to the nearest integer without any noise; the errors are fairly substantial, even when compared to the experimental errors in Table VIII. Thus merely the quantization by the ADC's leads to errors around 1% in the offsets and 0.3% in the gains. When only 2 poses were averaged, then increased variance in the noise rapidly led to increased errors. When 100 poses were averaged, the errors remained close to the truncation errors.

Another reason is that the closed-loop procedure is more sensitive to noise than the open-loop procedure. In the simulations of Table IX for the open-loop procedure, the simulated joint angles found from the jig poses have noise added to them with a variance of 0.005 radians. This table shows that open-loop calibration would also degrade if only 2 poses are averaged. For 2-pose averaging, the errors appear to be dominated by truncation plus output noise in the joint angles. For 100-pose averaging, the open-loop errors are considerably

TABLE IX
SIMULATION: EFFECTS OF NOISE AND AVERAGING ON OFFSET ERROR (RAD) AND GAIN ERROR ($\times 10^{-3}$ RAD/COUNT) FOR OPEN-LOOP CALIBRATION, A VARIANCE OF 0.005 RAD HAS BEEN ADDED TO THE PRESUMED CORRECT JOINT ANGLES

Method	Noise Level	Offset Error	Gain Error
Closed loop: Average 2 poses	truncation	0.009	0.004
	variance 1	0.023	0.011
	variance 2	0.047	0.022
	variance 4	0.092	0.042
Closed loop: Average 100 poses	variance 1	0.009	0.004
	variance 1	0.010	0.004
	variance 1	0.015	0.007
Open loop: Average 2 poses	truncation	0.018	0.009
	variance 1	0.018	0.009
	variance 2	0.019	0.009
	variance 4	0.029	0.014
Open loop: Average 100 poses	variance 1	0.003	0.002
	variance 2	0.004	0.002
	variance 4	0.004	0.002

less sensitive to larger variance noise in the potentiometer readings. With this sufficient averaging, which gives results close to the truncation error, the open-loop method is about 2-3 times more accurate than the closed-loop method (for a reasonable assumption about the fixture's accuracy). Boulet [6] applied the closed-loop approach to a simple double-loop mechanism for parallel actuation of a revolute joint, and also noticed a problem with noise sensitivity. A more complete characterization of the robustness properties of the closed-loop approach will be required to explain the sensitivity to pose selection and noise [1], [5], and will be a topic for future research.

The proposed method is related to the use of the ball bar recently proposed in [9], because the ends of each pair of arms can be considered to be connected by two spherical joints at a fixed distance. The difference from Driels (1993) is then that there are three "ball bars" in two kinematic loops instead of one. It is possible to calibrate each loop separately as in Driels (1993), but it was found for our data that the nonlinear optimizations did not converge to the correct answer. When the three pairwise distance constraints were used together, convergence was no problem. Simulations have so far been inconclusive about explaining the convergence problem, since for some pose sets calibrating just a single loop at a time converged well. In principle, it should be better to calibrate the loops simultaneously to take into account loop interaction, but the issue requires further study.

REFERENCES

[1] B. Armstrong, "On finding exciting trajectories for identification experiments involving systems with nonlinear dynamics," *Int. J. Robot. Res.*, vol. 8, no. 6, 1989, pp.28-48.
[2] D. J. Bennett and J. M. Hollerbach, "Closed-loop kinematic calibration of the Utah-MIT Hand," *Experimental Robotics 1—The First Int. Symp.*, 1990, pp. 539-552.
[3] ——, "Autonomous calibration of single-loop closed kinematic chains formed by manipulators with passive endpoint constraints," *IEEE Trans. Robot. and Automat.*, vol. 7, pp. 597-606, 1991.
[4] D. J. Bennett, J. M. Hollerbach, and D. Geiger, "Autonomous robot calibration for hand-eye coordination," *Int. J. Robot. Res.*, vol. 10, 1991, pp. 550-559.

[5] J. H. Borm and C. H. Menq, "Determination of optimal measurement configurations for robot calibration based on observability measure," *Int. J. Robot. Res.*, vol. 10, no. 1, 1991, pp. 51-63.
[6] B. Boulet, "Modeling and control of a robotic joint with in-parallel redundant actuators," McGill University, 1992,
[7] J. J. Craig, "Calibration of industrial robots," *Proc. 24th Int. Symp. on Indust. Robots*, 1993, pp. 889-893.
[8] J. Denavit and R. S. Hartenberg, "A kinematic notation for lower pair mechanisms based on matrices," *J. Appl. Mech.*, vol. 22, pp. 215-221, 1955.
[9] M. R. Driels, "Using passive end-point motion constraints to calibrate robot manipulators," *J. Dyn. Syst., Meas., Cont.*, vol. 115, pp. 560-565, 1993.
[10] M. R. Driels and U. S. Pathre, "Significance of observation strategy on the design of robot calibration experiments," *J. Robot. Syst.*, vol. 7, pp. 197-223, 1990.
[11] A. Goswami, A. Quaid, and M. Peshkin, "Identifying robot parameters using partial pose information," *IEEE Cont. Syst.*, vol. 13, no. 5, pp. 6-14, 1993.
[12] J. M. Hollerbach and D. Lokhorst, "Closed-loop kinematic calibration of the RSI 6-DOF hand controler," *IEEE Int. Conf. Robot. and Automat.*, 1993, pp. 2:142-148.
[13] M. Khoshzaban, F. Sassani, and P. D. Lawrence, "Autonomous kinematic calibration of industrial hydraulic manipulators," in *Robototics and Manufacturing*. New York: ASME Press, 1992, vol. 4, pp. 577-584.
[14] A. Nahvi, J. M. Hollerbach, and V. Hayward, "Closed-loop kinematic calibration of a parallel-drive shoulder joint," in *Proc. IEEE Intl. Conf. Robot. and Automat.*, 1994, pp. 407-412.
[15] W. S. Newman and D. W. Osborn, "A new method for kinematic parameter calibration via laser line tracking," in *Proc. IEEE Int. Conf. Robot. and Automat.*, 1993, pp. 2:160-165.
[16] R. P. Paul, *Robot Manipulators: Mathematics, Programming, and Control.* Cambridge, MA: MIT Press, 1981.
[17] R. P. Podhorodeski, "A screw theory based forward displacement solution for hybrid manipulators," in *Proc. 2nd Nat. Appl. Mechanisms and Robot. Conf.*, 1991, pp. IIIC-2.
[18] K. Schröer, "Theory of kinematic modelling and numerical procedures for robot calibration," in *Robot Calibration,* London: Chapman & Hall, 1993, pp. 157-196.
[19] C. Wampler and T. Arai, "Calibration of robots having kinematic closed loops using non-linear least-squares estimation," in *Proc. IFTOMM Symp.*, 1992, pp. 1:153-158.
[20] H. Zhuang, B. Li, Z. S. Roth, and X. Xie, "Self-calibration and mirror center offset elimination of a multi-beam laser tracking system," *Robot. and Autonomous Syst.*, vol. 9, pp. 255-269, 1992.
[21] H. Zhuang, L. Wang, and Z. Roth, "Simultaneous calibration of a robot and a hand-mounted camera," in *IEEE Intl. Conf. Robot. and Automat.*, 1993, pp. 2:149-154.

John M. Hollerbach received the B.S. in chemistry in 1968 and the M.S. in mathematics in 1969 from the University of Michigan, and the S.M. in 1975 and the Ph.D. in 1978 from MIT in computer science.

He is currently Professor of Computer Science at the University of Utah. From 1989-1994 he was the Natural Sciences and Engineering/Canadian Institute for Advanced Research Professor of Robotics at McGill University, jointly in the Departments of Mechanical Engineering and Biomedical Engineering. From 1982-1989 he was on the faculty of the Department of Brain and Cognitive Sciences and a member of the Artificial Intelligence Laboratory at MIT; from 1978-1982 he was a Research Scientist there. He has published many papers in the area of robotics and biological motor control, has co-authored the book *Model-Based Control of a Robot Manipulator* (MIT Press, 1988), and has co-edited the books *Robot Motion: Planning and Control* (MIT Press, 1982) and *Vision and Action: An Invitation to Cognitive Science, Vol. 2* (MIT Press, 1990).

In 1984 he received an NSF Presidential Young Investigator Award; in 1988 he was named a Fellow of the Canadian Institute for Advanced Research. He was the Program Chairman of the 1989 IEEE International Conference on Robotics and Automation, and a Member of the Administrative Committee of the IEEE Robotics and Automation Society from 1989-1993. He is a Technical Editor of the IEEE TRANSACTIONS ON ROBOTICS AND AUTOMATION, Treasurer of the IEEE/ASME *Journal of Microelectromechanical Systems*, and a Senior Editor of Presence: Teleoperators and Virtual Environments. Dr. Hollerbach is a Senior Member of IEEE.

David M. Lokhorst graduated in 1985 from the University of British Columbia in Vancouver, with a B.A.Sc. in engineering physics. In 1989, Mr. Lokhorst attended the University of Toronto, and studied under Dr. J. K. Mills, specializing in robot manipulator control systems. He graduated in 1990 with an M.A.Sc. in Mechanical Engineering.

He worked for Delta Projects Inc. in Calgary, Alberta, as a project engineer, designing innovative gas processing facilities using reverse osmosis membranes. Since 1991, Mr. Lokhorst has worked for RSI Research, Ltd., in Victoria, British Columbia, where he is now Chief Engineer. RSI Research, Ltd., produces remote-controlled machines, manipulators, and computer control systems for heavy industrial vehicles.